# Ultrahigh energy neutrinos and nonlinear QCD dynamics

Magno V. T. Machado

*High Energy Physics Phenomenology Group, GFPAE IF-UFRGS, CP 15051, CEP 91501-970, Porto Alegre/RS, Brazil*
*The Abdus Salam International Centre for Theoretical Physics (ICTP), Strada Costiera 11, 34014 Trieste, Italy*
*CERN TH Division, CH-1211 Genève 23, Switzerland*

(Received 19 February 2004; published 16 September 2004)

The ultrahigh energy neutrino-nucleon cross sections are computed taking into account different phenomenological implementations of the nonlinear QCD dynamics. Based on the color dipole framework, the results for the saturation model supplemented by the Dokshitzer-Gribov-Lipatov-Altarelli-Parisi (DGLAP) evolution as well as for the Balitskii-Fadin-Kuraev-Lipatov (BFKL) formalism in the geometric scaling regime are presented. They are contrasted with recent calculations using next-to-leading order DGLAP and unified BFKL-DGLAP formalisms.

DOI: 10.1103/PhysRevD.70.053008 PACS numbers: 13.15.+g, 12.38.Bx, 13.60.Hb

## I. INTRODUCTION

The inelastic interaction of neutrinos with nucleons is in general described by the QCD-improved parton model. In ultrahigh energy neutrino interactions one probes a kinematical region which is not accessible in the current collider experiments. It is known so far that these reactions can be sensitive to the domain for the usual Bjorken variable $x \simeq m_{W,Z}^2/E_\nu \sim 10^{-8}$ at $E_\nu \sim 10^{12}$ GeV and electroweak boson virtualities $Q^2 \sim m_{W,Z}^2 \approx 10^3$ GeV$^2$, where $m_{W,Z}$ are the boson masses. In contrast, in the current electron-proton collider DESY HERA the interactions are probed in the typical kinematical range $x \gtrsim 10^{-5}$ and $0 \leq Q^2 \lesssim 10^3$ GeV$^2$ (the variables $x$ and photon virtuality $Q^2$ are correlated, with small $x$ data associated with low virtualities). There, the measurements of the deep inelastic $ep$ scattering structure functions have put important constraints on parton distributions, mainly sea quarks and gluons, in the small $x$ region. In perturbative QCD these distributions are expected to grow as $x$ decreases, which has been strongly confirmed by HERA data. Therefore, in order to provide accurate predictions for the ultrahigh energy neutrino-nucleon cross sections, a precise extrapolation of the structure functions to the small $x$ and large $Q^2$ region probed in these interactions is needed.

In the usual QCD-improved parton model, the power growth of the parton distributions functions in very high neutrino energies leads consequently to a power increasing of the neutrino-nucleon total cross section, which in turn implies in a violation of unitarity at high energies. This issue is an outstanding theoretical challenge, which has produced intense work towards a complete understanding of the nonlinear (higher twist) QCD corrections in the high parton density regime at a fixed impact parameter (for a recent review, see [1], and references therein). At present, one has reliable estimates for the kinematical domain where nonlinear (saturation) effects should play an important role. Namely, below a typical transverse momentum scale $Q_{\rm sat}^2(x) \sim x^{-\lambda}$, the so-called saturation scale [2], the growth of parton (gluon) density is tamed towards the black-disk limit of the target. This slowdown of the gluon distribution function prevents the total cross section violating unitarity. An important prediction of the nonlinear QCD approaches is the property of geometric scaling [3] below the saturation scale, where the gluon density (and cross sections) scales with the saturation momentum, which grows with $1/x$ as a power. It has also been shown that such scaling survives even above the saturation regime [4–6]: the kinematical region has been estimated to be $Q_{\rm sat}^2(x) < Q^2 < Q_{\rm sat}^4(x)/\Lambda_{\rm QCD}^2$ relying on the BFKL equation [7] in the presence of saturation [4]. This feature has important consequences in the underlying QCD dynamics at the nucleus-nucleus accelerators RHIC and LHC and should pose strong constraints to the cross sections beyond current accelerator energies. Concerning high energy neutrino cross sections, there are estimates constrained by HERA data based on Dokshitzer-Gribov-Lipatov-Altarelli-Parisi (DGLAP) [8] and effects of Balitskii-Fadin-Kuraev-Lipatov (BFKL) [7] linear evolutions [9–14] as well as implementations of nonlinear QCD corrections [15]. The linear next-to-leading order (NLO) DGLAP and unified BFKL-DGLAP results are found to be consistent with each other presenting somewhat small deviations [14]. An interesting analytical calculation using an approximate DGLAP solution with initial conditions from a soft nonperturbative model has been recently reported in Ref. [16]. Saturation effects are shown to be quite small in a recent DGLAP analysis [13], whereas it was found a reduction in the cross section by a factor of 2 at $E_\nu \sim 10^{12}$ GeV considering the saturation model or screening effects via the Balitsky-Kovchegov equation [15]. Recently, it has been claimed in Ref. [17] that the geometric scaling property can lead to an enhancement of the neutrino-nucleon total cross section by an order of magnitude compared to the leading twist cross section and would lead it further to its unitarization.

 

In this work one presents estimates for the ultrahigh energy neutrino-nucleon cross sections, focusing on the saturation models which encode the physics of nonlinear QCD evolution in a phenomenological way. The main point is those models provides a suitable dynamical extrapolation to very high energies/virtualities in much contrast to the usual DGLAP based approaches, which are not *a priori* valid in that regime and are dependent on quark and gluon distributions also unknown (no constraint from accelerator data) in that kinematical limit. Based on the color dipole framework, the first one presents the result for the saturation model [18] supplemented by QCD evolution [19]. The original saturation model [18] was proposed for either low values of $Q^2 \lesssim 150$ GeV$^2$, whereas high energy neutrino interactions are sensitive to large virtualities $Q^2 \sim m_{W,Z}^2$. Therefore, it is necessary to perform calculations with complete QCD evolution. Furthermore, one computes estimates of the ultrahigh neutrino-nucleon cross section through an implementation of the dipole cross section considering BFKL formalism in the geometric scaling region [20]. In the last section, the numerical results for both cases are shown and contrasted with recent NLO DGLAP estimates and with unified BFKL-DGLAP formalism without saturation effects.

## II. NEUTRINO-NUCLEON CROSS SECTION

Deep inelastic neutrino scattering can proceed via $W^\pm$ or $Z^0$ exchanges. The first case corresponds to charged current (CC) and the second one to the neutral current (NC) interactions, respectively. The standard kinematical variables which describe the processes above are given by $s = 2m_N E_\nu$, $Q^2 = -q^2$, $x = Q^2/(2p\cdot q)$, and $y = (p\cdot q)/m_N E_\nu$. Here, $m_N$ is the nucleon mass, $E_\nu$ labels the neutrino energy, and $p$ and $q$ are the four momenta of the nucleon and of the exchanged boson, respectively. The usual Bjorken variable and the momentum transfer are usually labeled as $x$ and $Q^2$, whereas $s$ is the total center-of-mass energy squared. One assumes an isoscalar target $N = (p+n)/2$, which is a good approximation for the present purpose.

At high energies a quite successful framework to describe QCD interactions is provided by the color dipole formalism [21], which allows an all twist computation (in contrast with the usual leading twist approximation) of the structure functions. The physical picture of the interaction is the deep inelastic scattering at low $x$ viewed as the result of the interaction of a color $q\bar{q}$ dipole which the gauge bosons fluctuate to with the nucleon target. The interaction is modeled via the dipole-target cross section, whereas the boson fluctuation in a color dipole is given by the corresponding wave function. The deep inelastic scattering structure functions for neutrino-nucleon scattering in the dipole picture read as [15,17]

$$F_{T,L}^{\rm CC,NC}(x,Q^2) = \frac{Q^2}{4\pi^2}\int d^2\boldsymbol{r}\int_0^1 dz|\psi_{T,L}^{W^\pm,Z^0}|^2\sigma_{\rm dip}, \qquad (1)$$

where $\boldsymbol{r}$ denotes the transverse size of the color dipole, $z$ the longitudinal momentum fraction carried by a quark, and $\psi_{T,L}^{W,Z}$ are proportional to the wave functions of the (virtual) charged or neutral gauge bosons corresponding to their transverse or longitudinal polarization ($F_2 = F_T + F_L$). Explicit expressions for the boson ($W^\pm$ and $Z^0$) wave functions squared are as follows [15]:

$$|\psi_T^{W^\pm}(r,z,Q^2)|^2 = \frac{6}{\pi^2}[z^2+(1-z)^2]\varepsilon^2K_1^2(\varepsilon\boldsymbol{r}), \qquad (2)$$

$$|\psi_L^{W^\pm}(r,z,Q^2)|^2 = \frac{24}{\pi^2}z^2(1-z)^2Q^2K_0^2(\varepsilon\boldsymbol{r}), \qquad (3)$$

$$|\psi_T^{Z^0}(r,z,Q^2)|^2 = \frac{3}{2\pi^2}K_W[z^2+(1-z)^2]\varepsilon^2K_1^2(\varepsilon\boldsymbol{r}), \quad (4)$$

$$|\psi_L^{Z^0}(r,z,Q^2)|^2 = \frac{6}{\pi^2}K_W z^2(1-z)^2Q^2K_0^2(\varepsilon\boldsymbol{r}), \qquad (5)$$

where one defines the auxiliary variable $\varepsilon = z(1-z)Q^2$ and $K_{0,1}(x)$ are the McDonald's functions. Here, $K_W = (L_u^2 + L_d^2 + R_u^2 + R_d^2)$ and the chiral couplings are expressed as functions of the Weinberg angle $\theta_W$ as follows:

$$L_u = 1 - \tfrac{4}{3}\sin^2\theta_W, \qquad L_d = -1 + \tfrac{2}{3}\sin^2\theta_W, \qquad (6)$$

$$R_u = -\tfrac{4}{3}\sin^2\theta_W, \qquad R_d = \tfrac{2}{3}\sin^2\theta_W. \qquad (7)$$

Following Ref. [15], one considers only four flavors $(u,d,s,c)$ and assumes them massless, whereas it has been shown [14] that heavy quarks $(b,t)$ give relatively small contribution. Moreover, the color dipoles contributing to Cabibbo favored transitions are $u\bar{d}$ $(d\bar{u})$, $c\bar{s}$ $(s\bar{c})$ for CC interactions and $u\bar{u}$, $d\bar{d}$, $c\bar{c}$, and $s\bar{s}$ for NC interactions. In our further numerical calculations using the dipole framework, we use the structure function $F_3^{\rm CC,NC}$ given by the usual leading order (LO) DGLAP expressions [22], despite their contributions to be small for the present purpose.

The total CC (NC) neutrino-nucleon cross sections as a function of the neutrino energy are given by the integration over available phase space at the given neutrino energy. They read as

$$\sigma_{(\nu,\bar{\nu})}^{\rm CC,NC}(E_\nu) = \int_{Q^2_{\rm min}}^s dQ^2\int_{Q^2/s}^1 dx\frac{1}{xs}\frac{\partial^2\sigma_{(\nu,\bar{\nu})}^{\rm CC,NC}}{\partial x\partial y}, \qquad (8)$$

where $y = Q^2/(xs)$ and a minimum value $Q^2_{\rm min}$ (of the order of a few GeV's) on $Q^2$ is introduced in order to stay in the deep inelastic region.

In the present work we are interested in the ultrahigh energy neutrinos ($E_\nu \gg 10^7$ GeV), where the valence quark contribution stays constant and physics is driven by sea quark contributions. In this region, we will use the available phenomenology on nonlinear QCD evolutions to study saturation effects in the neutrino-nucleon cross section.

The dipole cross section $\sigma_{\rm dip}$, describing the dipole-nucleon interaction, is substantially affected by saturation effects at dipole sizes $\boldsymbol{r} \gtrsim 1/Q_{\rm sat}$. Here, we follow the saturation model [18], which interpolates between the small and large dipole configurations, providing color transparency behavior, $\sigma_{\rm dip} \sim \boldsymbol{r}^2$, as $\boldsymbol{r} \to 0$ and constant behavior, $\sigma_{\rm dip} \sim \sigma_0$, at large dipoles. The transition is rendered by the saturation phenomenon. The parametrization for the dipole cross section takes the eikonal-like form,

$$\sigma_{\rm dip}(\tilde{x}, \boldsymbol{r}^2) = \sigma_0\left[1 - \exp\left(-\frac{Q_s^2(x)\boldsymbol{r}^2}{4}\right)\right](1-\tilde{x})^7, \qquad (9)$$

where the saturation scale $Q_s^2(x) = (x_0/\tilde{x})^\lambda$ defines the onset of the saturation effects. As known, most of the contribution to the ultrahigh energy neutrino cross section comes from very small $x \approx m_{W,Z}^2/2m_N E_\nu$ and therefore a sizable part of the contributions is in the geometric scaling region or even in the saturation region [17]. The parameters ($\sigma_0$, $\lambda$, and $x_0$) were obtained from a fit to the HERA data [18]. The variable $\tilde{x} = x(1 + 4m_f^2/Q^2)$ gives a suitable transition to the photoproduction region. The saturation model has been used to compute the neutrino-nucleon cross section in Ref. [15]. There, it was shown that the saturation model does not include complete DGLAP QCD evolution at high virtualities and tends to be therefore lower than other calculations, probably meaning that it is rather incomplete and inaccurate in the high $Q^2$ region.

Recently, a new implementation of the model including QCD evolution [19] [labeled the Bartels-Golec-Biernat-Kowalski (BGBK) model] has appeared. Now, the dipole cross section depends on the gluon distribution as

$$\sigma_{\rm dip} = \sigma_0\left[1 - \exp\left(-\frac{\pi^2\boldsymbol{r}^2\alpha_s(\mu^2)\tilde{x}G(\tilde{x}, \mu^2)}{3\sigma_0}\right)\right], \qquad (10)$$

where the initial condition at $\mu^2 = 1\ \text{GeV}^2$ is $xG = A_g x^{-\lambda_g}(1-x)^{5.6}$ and $\mu^2 = C/\boldsymbol{r}^2 + \mu_0^2$. The phenomenological parameters are determined from a fit to small $x$ HERA data. The function $G(x, \mu^2)$ is evolved with the leading order DGLAP evolution equation for the gluon density with initial scale $Q_0^2 = 1\ \text{GeV}^2$. The improvement preserves the main features of the low $Q^2$ and transition regions, while providing QCD evolution in the large $Q^2$ domain.

Despite the saturation model to be very successful in describing HERA data, its functional form is only an approximation motivated by the Glauber-Mueller formula, which does not include impact parameter dependence. On the other hand, an analytical expression for the dipole cross section can be obtained within the BFKL formalism. Currently, intense theoretical studies have been performed towards an understanding of the BFKL approach in the border of the saturation region [4,6]. In particular, the dipole cross section has been calculated in both LO [7] and NLO BFKL [23] approaches in the geometric scaling region [24]. It reads as

$$\sigma_{\rm dip} = \sigma_0[\boldsymbol{r}^2 Q_{\rm sat}^2(x)]^{\gamma_{\rm sat}} \exp\left[-\frac{\ln^2(\boldsymbol{r}^2 Q_{\rm sat}^2)}{2\beta\bar{\alpha}_s Y}\right], \qquad (11)$$

where $\sigma_0 = 2\pi R_p^2$ ($R_p$ is the proton radius) is the overall normalization and the power $\gamma_{\rm sat}$ is the (BFKL) saddle point in the vicinity of the saturation line $Q^2 = Q_{\rm sat}^2(x)$ (the anomalous dimension is defined as $\gamma = 1 - \gamma_{\rm sat}$). As usual in the BFKL formalism, $\bar{\alpha}_s = N_c\alpha_s/\pi$, $\beta \simeq 28\zeta(3)$, and the notation $Y = \ln(1/x)$. The quadratic diffusion factor in the exponential gives rise to the scaling violations. Equation (11) has been used in Ref. [17] to show an estimation of the enhancement factor (about a factor of 10) in the ultrahigh neutrino-nucleon cross section in contrast with the usual leading twist calculations.

The dipole cross section in Eq. (11) does not include an extrapolation from the geometric scaling region to the saturation region. This has been recently implemented in Ref. [20], where the dipole amplitude $\mathcal{N}(x, \boldsymbol{r}) = \sigma_{\rm dip}/2\pi R_p^2$ was constructed to smoothly interpole between the limiting behaviors analytically under control: the solution of the BFKL equation for small dipole sizes, $\boldsymbol{r} \ll 1/Q_{\rm sat}(x)$, and the Levin-Tuchin law [25] for larger ones, $\boldsymbol{r} \gg 1/Q_{\rm sat}(x)$. A fit to the structure function $F_2(x, Q^2)$ was performed in the kinematical range of interest, showing that it is not very sensitive to the details of the interpolation. The dipole cross section was parametrized as follows:

$$\sigma_{\rm dip} = \sigma_0 \begin{cases} \mathcal{N}_0\left(\frac{\boldsymbol{r}Q_{\rm sat}}{2}\right)^{2\{\gamma_{\rm sat} + [\ln(2/\boldsymbol{r}Q_{\rm sat})/\kappa\lambda Y]\}}, & (\boldsymbol{r}Q_s \le 2), \\ 1 - \exp^{-a\ln^2(b\boldsymbol{r}Q_{\rm sat})}, & (\boldsymbol{r}Q_s > 2), \end{cases}$$

where the expression for $\boldsymbol{r}Q_{\rm sat}(x) > 2$ (saturation region) has the correct functional form, as obtained either by solving the Balitsky-Kovchegov equation [26], or from the theory of the Color Glass Condensate (CGC) [27]. Hereafter, we label the model above by CGC. The coefficients $a$ and $b$ are determined from the continuity conditions of the dipole cross section at $\boldsymbol{r}Q_{\rm sat}(x) = 2$. The coefficients $\gamma_{\rm sat} = 0.63$ and $\kappa = 9.9$ are fixed from their LO BFKL values. Our further calculations will use the parameters $R_p = 0.641$ fm, $\lambda = 0.253$, $x_0 = 0.267 \times 10^{-4}$, and $\mathcal{N}_0 = 0.7$, which give the best fit result. A large $x$ threshold factor $(1-x)^5$ will also be considered.

## III. RESULTS AND DISCUSSION

In what follows, one computes the ultrahigh energy CC and NC neutrino-nucleon cross sections using the

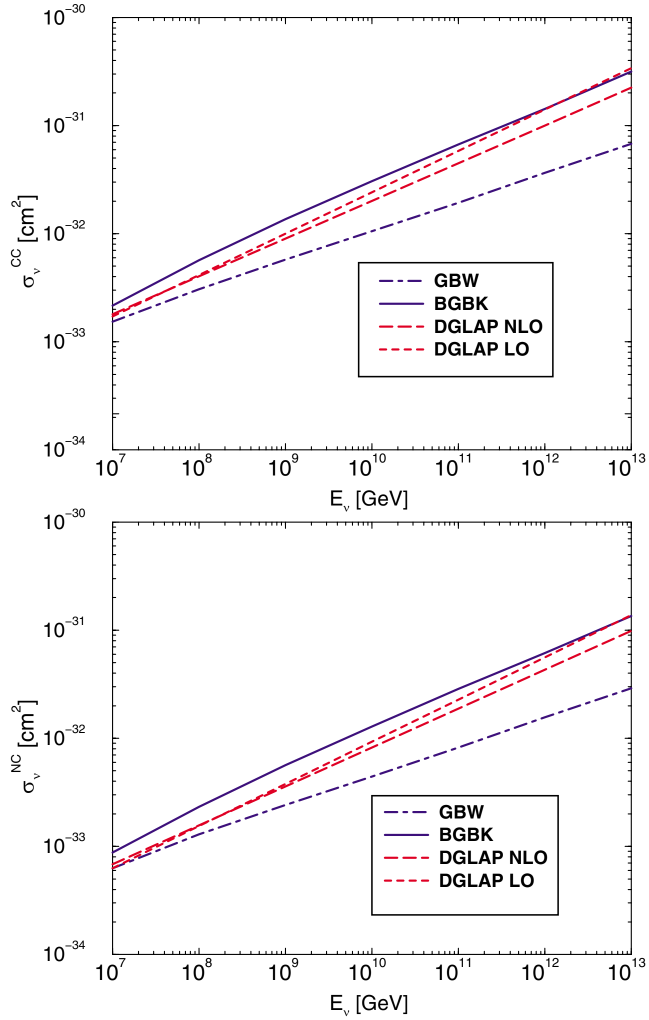


FIG. 1 (color online). The $\nu N$ charged current (a) and neutral current (b) as a function of neutrino energy. The curves correspond to the results for the GBW saturation model (dot-dashed curves) and the BGBK model (solid lines). The LO and NLO DGLAP results are represented by dashed and long-dashed curves, respectively.

different models containing saturation effects. In Fig. 1 one presents the results for the saturation model Golec-Biernat-Wusthoff (GBW), the BGBK model, and also one includes a DGLAP calculation. The result for the saturation model (dot-dashed lines) has been recently computed in Ref. [15], which we reproduce here. The introduction of the DGLAP evolution in the saturation model enhances the cross section by a factor of 3 or even more at $E_\nu \sim 10^{12}$ GeV. This is shown by the BGBK curves (solid lines). It should be noticed that the power growth for the saturation model is milder than the BGBK model and it gives an upper limit for the role played by saturation effects in the cross section. It should be emphasized that this comment refers to the comparison between the phenomenological saturation model and its version including the DGLAP evolution. Namely, other nonlinear QCD approaches can give a larger amount of saturation in the same kinematical regime and the phenomenological saturation model probably is inaccurate in this region. For sake of completeness, the DGLAP results (LO and NLO) are also presented. For this purpose, we follow the calculations in Ref. [13], where a detailed analysis of the NLO corrections to neutrino-nucleon cross sections was performed. The BGBK model has an energy dependence at ultrahigh energy neutrinos similar to the NLO DGLAP (long-dashed lines) for $E_\nu \gtrsim 10^9$ GeV.

In order to investigate the BFKL physics in the geometric scaling region, we use the recent fit to the dipole cross section presented in Ref. [20] (the CGC model), which encodes the BFKL formalism in the geometric scaling regime and an interpolation to the saturation domain, as presented in the last section. It should be noticed that an analysis including the DGLAP evolution in the fit would be timely. However, as the CGC model produces an "effective" anomalous dimension, i.e., $\gamma_{\rm eff}(x, \boldsymbol{r}Q_{\rm sat}) \equiv \gamma_{\rm sat} + (\kappa\lambda Y)^{-1}\ln(4/\boldsymbol{r}^2 Q_{\rm sat}^2)$ [20] far from the geometric scaling region $\boldsymbol{r}^2 Q_{\rm sat}^2(x) \ll 1$, which is closer to the DGLAP one, the estimate presented here would not be strongly spoiled by the QCD evolution. The results for the CGC model (solid lines) are presented in Fig. 2, contrasted with the NLO DGLAP calculation (dashed lines) and also with the unified BFKL-DGLAP formalism (dot-dashed lines), which embodies nonleading $\ln(1/x)$ contributions [14]. The latter incorporates both the $\ln(1/x)$ BFKL resummation and the complete LO DGLAP evolution, with the dominant nonleading $\ln(1/x)$ contributions resummed to all orders. The result found for the CGC model is quite similar to both DGLAP and unified BFKL-DGLAP formalisms in the range of energy considered here. It has not observed any enhancement in the neutrino-nucleon cross section in comparison with the leading twist DGLAP calculation, even at very high energies of order $E_\nu \sim 10^{12}$ GeV. This fact is in disagreement with Ref. [17], where it has been shown that the geometric scaling leads to an enhancement of the neutrino-nucleon total cross section by an order of magnitude versus the leading twist cross section. We also verify that at $E_\nu \gtrsim 10^{11}$ GeV the power on energy starts to slow down and it should be increasingly smoother (logarithmic growth) at higher energies. This expected change of behavior on the energy of the cross section is estimated to be reached at $E_\nu \sim 10^{18}$ GeV in Ref. [17], suppressing the cross section compared to the leading twist result.

We can qualitatively understand the result above analyzing the ratio between the dipole cross section for BFKL and DGLAP approaches in the geometric scaling regime. As discussed before, the ultrahigh energy neutrino cross section is sensitive to the kinematical

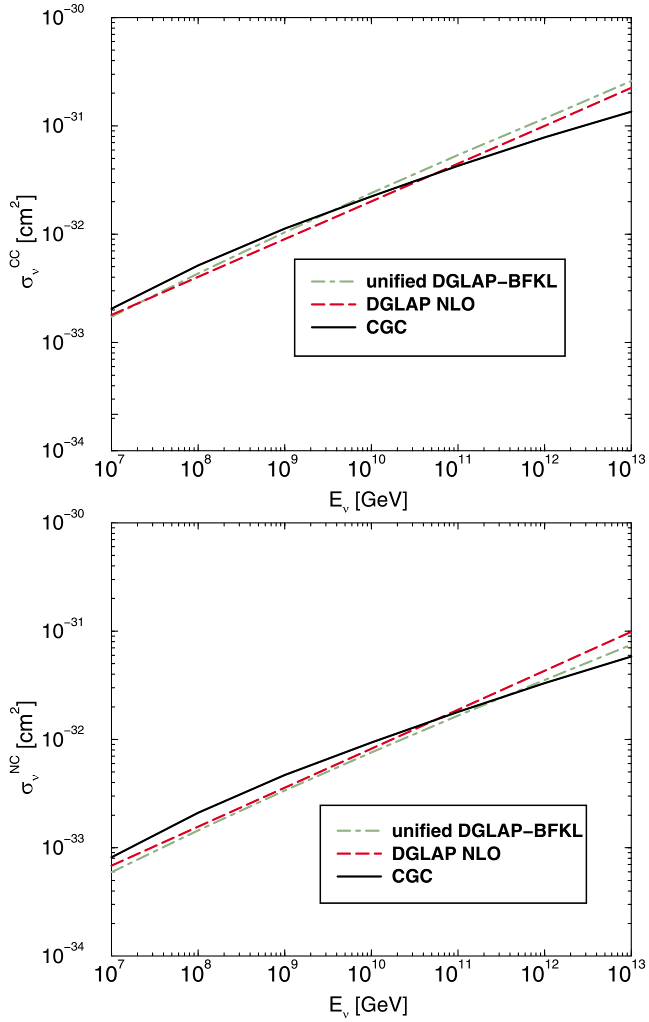


FIG. 2 (color online). The $\nu N$ charged current (a) and neutral current (b) as a function of neutrino energy. The solid curves correspond to the results for the CGC model. The NLO DGLAP result is represented by the dashed curves and the unified BFKL-DGLAP formalism by the dot-dashed curves, respectively.

region of small $x \sim m_{W,Z}^2/E_\nu$ and high $Q^2 \sim m_{W,Z}^2$. Concerning DGLAP formalism, in such a region we are in the double logarithmic approximation (DLA) limit. Concerning the nonlinear QCD approaches, at the vicinity of saturation, the DLA saddle point is no longer equal to 1, but it was found to be $\gamma_{\mathrm{sat}}^{\mathrm{DLA}} \simeq 1/2$ [4,5,28]. The ratio of the cross section in the geometric scaling region is given by

$$R_{\mathrm{scal}} \sim \frac{[\boldsymbol{r}^2 Q_{\mathrm{sat}}^2]^{\gamma_{\mathrm{sat}}^{\mathrm{BFKL}}}}{[\boldsymbol{r}^2 Q_{\mathrm{sat}}^2]^{\gamma_{\mathrm{sat}}^{\mathrm{DLA}}}} \simeq \left[\frac{Q_{\mathrm{sat}}^2}{m_{W,Z}^2}\right]^{(\gamma_{\mathrm{sat}}^{\mathrm{BFKL}} - \gamma_{\mathrm{sat}}^{\mathrm{DLA}})} \sim \mathcal{O}(1),$$

where we have disregarded the diffusion factor in the BFKL expression and considered $\boldsymbol{r}^2 \simeq 1/Q^2 \sim 1/m_{W,Z}^2$. The result $R_{\mathrm{scal}} \simeq 1$ leads to similar results between the all twist and leading twist calculation in the geometric scaling region. In fact, there is room for a slight suppression since $(\gamma_{\mathrm{sat}}^{\mathrm{BFKL}} - \gamma_{\mathrm{sat}}^{\mathrm{DLA}}) \simeq 0.13$ and $Q_{\mathrm{sat}}^2/m_{W,Z}^2 < 1$. On the other hand, the argument in Ref. [17] is exactly true in the comparison between CGC and GBW models. In this case, as we will discuss in what follows, $\gamma_{\mathrm{sat}}^{\mathrm{GBW}} = 1$ in the geometric scaling region and a sizable enhancement between CGC and GBW is really observed.

The qualitative analysis presented above can also help us to understand the enhancement of the BGBK model (with DGLAP evolution) in relation to the GBW saturation model. We can think in an effective "anomalous dimension" for the saturation model in the geometric scaling regime: from Eq. (9), $\sigma_{\mathrm{dip}}^{\mathrm{GBW}} \simeq \boldsymbol{r}^2 Q_{\mathrm{sat}}^2/4$ and then one verifies that $\gamma_{\mathrm{sat}}^{\mathrm{GBW}} = 1$. In this case, the ratio now reads as

$$R_{\mathrm{scal}} = \frac{\sigma_{\mathrm{dip}}(\mathrm{BGBK})}{\sigma_{\mathrm{dip}}(\mathrm{GBW})} \sim \left[\frac{Q_{\mathrm{sat}}^2}{m_{W,Z}^2}\right]^{(\gamma_{\mathrm{sat}}^{\mathrm{DLA}} - \gamma_{\mathrm{sat}}^{\mathrm{GBW}})} \gg 1, \qquad (12)$$

whereas at lower energies (beyond the geometric scaling regime) the DGLAP anomalous dimension takes the usual value and the ratio is closer to 1, as expected.

As a summary, we have presented the results for the ultrahigh energy neutrino cross section considering the current phenomenology on nonlinear QCD dynamics, which play an important role in the correct extrapolation to the regime of very high gluon density. The saturation model with QCD evolution was studied as well as the physics of BFKL dynamics at the geometric scaling region. The latter presents suppression in the cross section at $E_\nu \gtrsim 10^{12}$ GeV, whereas the BGBK model is consistent with NLO DGLAP calculations. An outstanding advantage in the color dipole framework is the possibility to provide analytical expressions for the extrapolation to ultrahigh energies, towards the black limit of the nucleon target. This cannot be taken into account in a leading twist approach as the QCD-improved parton model. Then these saturation (all twist) approaches play an important role, since a precise knowledge about the neutrino interactions and production rates is essential for estimating background, expected fluxes, and detection probabilities [14,29]. In particular, reliable estimates for ultrahigh energy neutrino cross section are strongly needed for the planned experiments [30] to detect them via nearly horizontal air showers in the Earth's atmosphere, as discussed in [16].

## ACKNOWLEDGMENTS

The author is grateful for the warm hospitality and financial support of the High Energy Group in The Abdus Salam International Centre for Theoretical Physics (ICTP) at Trieste and CERN Theory Division at Geneve, where part of this work was performed. The author also would like to thank Alexei Smirnov

(ICTP, Trieste) and Krysztof Kutak (II Institute for Theoretical Physics, Hamburg) for helpful discussions. This work was partially supported by CNPq, Brazil.

[1] N. Armesto, Acta Phys. Pol. B **35**, 213 (2004).
[2] L.V. Gribov, E. M. Levin, and M. G. Ryskin, Phys. Rep. **100**, 1 (1983); A. H. Mueller, Nucl. Phys. **B558**, 285 (1999).
[3] A. M. Staśto, K. Golec-Biernat, and J. Kwieciński, Phys. Rev. Lett. **86**, 596 (2001).
[4] E. Iancu, K. Itakura, and L. McLerran, Nucl. Phys. **A708**, 327 (2002).
[5] J. Kwieciński and A. M. Staśto, Phys. Rev. D **66**, 014013 (2002).
[6] S. Munier and S. Wallon, Eur. Phys. J. C **30**, 359 (2003).
[7] L. N. Lipatov, Sov. J. Nucl. Phys. **23**, 338 (1976); E. A. Kuraev, L. N. Lipatov, and V. S. Fadin, JETP Lett. **45**, 1999 (1977); I. I. Balitskii and L. N. Lipatov, Sov. J. Nucl. Phys. **28**, 822 (1978).
[8] V. N. Gribov and L. N. Lipatov, Sov. J. Nucl. Phys. **15**, 438 (1972); G. Altarelli and G. Parisi, Nucl. Phys. **B126**, 298 (1977); Yu. L. Dokshitzer, Sov. Phys. JETP **46**, 641 (1977).
[9] D. A. Dicus, S. Kretzer, W.W. Repko, and C. Schmidt, Phys. Lett. B **514**, 103 (2001).
[10] R. Gandhi, C. Quigg, M.H. Reno, and I. Sarcevic, Astropart. Phys. **5**, 81 (1996); Phys. Rev. D **58**, 093009 (1998).
[11] M. H. Reno, I. Sarcevic, G. Sterman, M. Stratmann, and W. Vogelsang, eConf No. C010630:P508, 2001.
[12] M. Glück, S. Kretzer, and E. Reya, Astropart. Phys. **11**, 327 (1999).
[13] R. Basu, D. Choudhury, and S. Majhi, J. High Energy Phys. 10 (2002) 012.
[14] J. Kwieciński, A. D. Martin, and A. M. Staśto, Phys. Rev. D **59**, 093002 (1999).
[15] K. Kutak and J. Kwieciński, Eur. Phys. J. C **29**, 521 (2003).
[16] R. Fiore *et al.*, Phys. Rev. D **68**, 093010 (2003).
[17] J. Jalilian-Marian, Phys. Rev. D **68**, 054005 (2003).
[18] K. Golec-Biernat and M. Wüsthoff, Phys. Rev. D **59**, 014017 (1999); **60**, 114023 (1999).
[19] J. Bartels, K. Golec-Biernat, and H. Kowalski, Phys. Rev. D **66**, 014001 (2002).
[20] E. Iancu, K. Itakura, and S. Munier, Phys. Lett. B **590**, 199 (2004).
[21] A. H. Mueller, Nucl. Phys. **B335**, 115 (1990); N. N. Nikolaev and B. G. Zakharov, Z. Phys. C **49**, 607 (1991).
[22] B. Humpert and W. L. van Neerven, Nucl. Phys. **B184**, 225 (1981).
[23] V. S. Fadin and L. N. Lipatov, Phys. Lett. B **429**, 127 (1998); G. Camici and M. Ciafaloni, Phys. Lett. B **430**, 349 (1998).
[24] A. H. Mueller and D. N. Triantafyllopoulos, Nucl. Phys. **B640**, 331 (2002); D. N. Triantafyllopoulos, Nucl. Phys. **B648**, 293 (2003); A. H. Mueller, Nucl. Phys. **A724**, 223 (2003).
[25] E. Levin and K. Tuchin, Nucl. Phys. **B573**, 833 (2000).
[26] I. Balitsky, Nucl. Phys. **B463**, 99 (1996); Yu. V. Kovchegov, Phys. Rev. D **60**, 034008 (1999); **61**, 074018 (2000).
[27] E. Iancu and R. Venugopalan, hep-ph/0303204.
[28] K. Golec-Biernat, L. Motyka, and A. M. Staśto, Phys. Rev. D **65**, 074037 (2002).
[29] A. M. Staśto, Int. J. Mod. Phys. A **19**, 317 (2004).
[30] A. Kusenko and T. J. Weiler, Phys. Rev. Lett. **88**, 161101 (2002); A. Kusenko, hep-ph/0203002.